[redacted]

NASA TECHNICAL MEMORANDUM

NASA TM X-724

NASA TM X-724

REMOVED FROM CATEGORY 7
AUTHORITY- MEMO FROM
DROEKA TO LEBOW DATED [redacted]

JUN - 9 1966

DECLASSIFIED- AUTHORITY
US: 1286 DROEKA TO LEBOW
MEMO DATED
6/8/66

Declassified by authority of NASA
Classification Change Notices No. 67
Dated ** 6/29/66

EXPERIMENTAL HYDROGEN-FLUORINE ROCKET PERFORMANCE AT LOW PRESSURES AND HIGH AREA RATIOS

by Carl A. Aukerman and Bruce E. Church;
Lewis Research Center,
Cleveland, Ohio

NATIONAL AERONAUTICS AND SPACE ADMINISTRATION • WASHINGTON, D. C. • SEPTEMBER 1963

[redacted]

[redacted]

TECHNICAL MEMORANDUM X-724

EXPERIMENTAL HYDROGEN-FLUORINE ROCKET PERFORMANCE AT LOW PRESSURES AND HIGH AREA RATIOS

By Carl A. Aukerman and Bruce E. Church

Lewis Research Center
Cleveland, Ohio

[redacted]

NATIONAL AERONAUTICS AND SPACE ADMINISTRATION

[redacted]

NATIONAL AERONAUTICS AND SPACE ADMINISTRATION

TECHNICAL MEMORANDUM X-724

EXPERIMENTAL HYDROGEN-FLUORINE ROCKET PERFORMANCE AT LOW PRESSURES AND HIGH AREA RATIOS*

By Carl A. Aukerman and Bruce E. Church

SUMMARY

33325

The performance of hydrogen and fluorine was evaluated in an altitude test facility at low chamber pressures in rocket engines having area-ratio-100 exhaust nozzles of three lengths. Chamber pressure ranged from 60 to 10 pounds per square inch absolute and mixture ratio from 12 to 6 percent hydrogen. The nominal thrust was 1400 pounds at a chamber pressure of 60 pounds per square inch absolute.

A conical nozzle of 15° half-angle produced a vacuum thrust coefficient of approximately 98 percent of one-dimensional theoretical equilibrium and was relatively insensitive to changes in chamber pressure. This value represents near-equilibrium nozzle performance with respect to internal flow characteristics. The maximum vacuum specific impulse measured was 465 pound-seconds per pound. A conical nozzle of 25° half-angle and a bell-shaped nozzle contoured to 70 percent of the length of the 15° conical had thrust coefficients near frozen expansion for the conditions tested. The lower performance of the two shorter nozzles was attributed to the failure of the dissociated exhaust products to recombine at higher expansion rates.

Author

INTRODUCTION

The drive for more ambitious missions and larger payloads in the exploration of space places greater emphasis on improved propulsion systems. Mission studies reported in references 1 and 2 show the advantages in payload increase that can be realized with existing boosters by using high-energy propellants in the upper stages. Reference 3 shows that missions requiring long coast periods in space do not alter the situation significantly. In each of these studies, the propellant combination of fluorine and hydrogen offered several advantages toward the achievement of reliable high-performance systems and emerged as the most favorable of the various combinations. Most notable of the advantages of this combination are its low hydrogen requirements, hypergolic nature, and extremely high specific impulse. Minimizing hydrogen requirements is important because of the low density of hydrogen and the resulting high propellant tankage volume and weight. The hypergolic nature of hydrogen and fluorine should provide nearly

*Title, Unclassified.

perfect ignition and restart capabilities under all conditions. When these features are coupled with a low-chamber-pressure, pressure-fed propellant system, the resulting vehicle can be a simple, reliable, lightweight, high-energy propulsive device.

Although the theoretical shifting-equilibrium performance of hydrogen and fluorine is higher than that of any other stable chemical propellant combination, the ability to approach theoretical shifting equilibrium expansion in an exhaust nozzle as opposed to theoretical frozen flow has not before been clearly established by experiment. The difference in specific impulse between the extreme flow conditions can be as great as 86 seconds, or 18 percent, in a nozzle with an area ratio of 100 at a chamber pressure of 60 pounds per square inch absolute. The importance of this difference in terms of potential vehicle performance and payload is significant, and knowledge of the experimental performance of hydrogen and fluorine in conventional nozzles and the determination of nozzle design parameters to promote recombination become vital requirements.

Some work in hydrogen-fluorine expansion nozzles has been done at the Lewis Research Center at area ratios of 25 and 100, but, because of facility limitations, chamber pressures were limited to the range 200 to 725 pounds per square inch absolute (ref. 4). The program discussed herein included three nozzles with area ratios of 100 operated at chamber pressures from 60 to 10 pounds per square inch absolute with a nominal thrust level of 1400 pounds at the high chamber pressure. The objectives were to define performance with large-area-ratio nozzles at low chamber pressures and to determine the effect of nozzle shape on the recombination process as it is described by thrust coefficient and impulse efficiency.

Mixture ratio was varied from 12 to 6 percent hydrogen, but, in general, emphasis was placed at approximately 11 percent. Studies have indicated optimum conditions between 8 and 11 percent hydrogen depending on the detailed mission requirements. Tankage and weight problems favor the lower hydrogen percentage, but peak performance and cooling considerations favor the fuel-rich condition.

The three nozzles evaluated were a cone of 15° half-angle, a cone of 25° half-angle, and a bell-shaped nozzle contoured to 70 percent of the length of the 15° conical one. The program was conducted in an altitude test facility, and a zero-flow, second-throat exhaust diffuser was employed to provide additional altitude simulation.

The symbols used throughout the report are defined in appendix A, and the method of calculation of experimental and theoretical values is discussed in appendix B.

APPARATUS

Facility

A schematic drawing of the test section of the altitude facility that was used for this program is shown in figure 1. This facility is capable of altitude simulation to approximately 100,000 feet, and ambient pressures from 32 to 36

pounds per square foot absolute were maintained during rocket operation. A second-throat, zero-flow exhaust diffuser was utilized in addition to the rotating exhausters of the altitude facility to attain minimum pressures of 0.01 to 0.06 pound per square inch absolute, which were required for full expansion of the exhaust gases in the large area ratio experimental rocket nozzles. Information from reference 5 was used to design the exhaust diffuser shown in the following sketch:

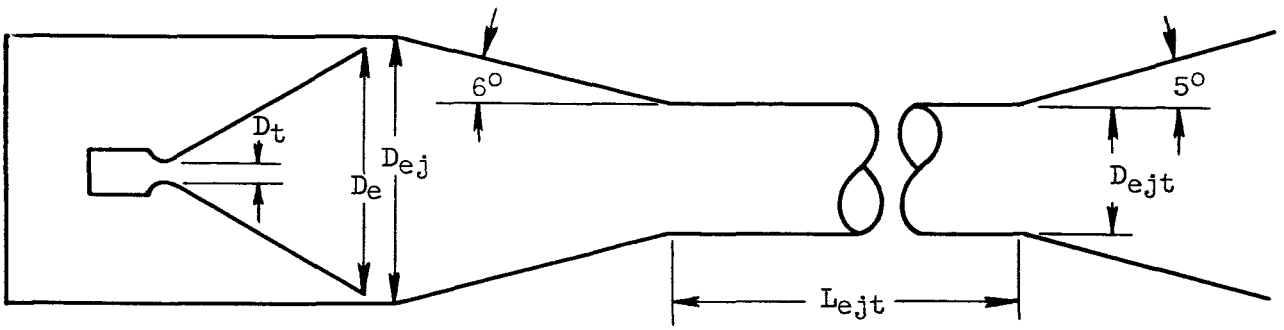

The geometric relations that resulted are

$$A_{ej}/A_t = (D_{ej}/D_t)^2 = 107.3$$

$$A_{ej}/A_{ejt} = (D_{ej}/D_{ejt})^2 = 2.18$$

$$L_{ejt}/D_{ejt} = 5.28$$

This diffuser design provided the required altitude for the 15° conical nozzle, but, with the 25° conical and 70 percent contour nozzles, the diffuser would not start or operate at lower chamber pressures. The starting and operating difficulties with the latter two nozzles were attributed to differences in the nozzle-exit gas conditions and possibly to the effect of dissociation on the isentropic exponent γ.

A pressure-tight capsule attached to the ejector completely surrounded the thrust-chamber nozzle assembly and load cell. This simplified thrust measurement by preventing additional force components on the engine from pressure differentials acting on ungrounded surface areas such as seals and bellows. To prevent the accumulation of an explosive atmosphere in the exhaust equipment, the excess hydrogen in the rocket exhaust products was mixed with air bled around the diffuser exit and ignited by a small hydrogen-air torch that burned continuously.

Propellant Supply System

Fuel system. - Gaseous hydrogen was fed to the engine directly from a supply trailer located outside the building. Flow rates were determined from measurements of temperature, pressure, and pressure differential at an orifice plate located in the hydrogen line near the engine inside the test chamber.

Oxidant system. - Liquid fluorine was supplied to the engine from a 2-cubic-foot Dewar located in the altitude test section. The Dewar, the supply lines to the capsule, and the Venturi flowmeter were encased in a jacket containing liquid nitrogen regulated to sea-level pressure. This process controlled fluorine temperature and density and simplified oxidant flow measurement. Fluorine flow rates were determined by measuring the pressure differential across a calibrated Venturi flowmeter. Helium was used to pressurize the fluorine tank to approximately 400 pounds per square inch absolute.

Chambers and Nozzles

The basic combustion-chamber configuration had a 12-square-inch throat area (3.91 in. diam.), a chamber contraction ratio of 1.9, and a characteristic length L^* of 21.0 inches. The chambers were of a heat-sink design and had a zirconium oxide coating on the inside to produce a thermal lag to increase the time of operation. This coating eventually eroded away in spots and required replacement.

The three rocket exhaust nozzles used for this investigation are pictured, with chambers attached, in figure 2. A cone-shaped nozzle with a 15° half-angle was used as the standard for comparison. Effects of nozzle shape on performance were studied with a 25° conical nozzle and a bell-shaped nozzle contoured to 70 percent of the length of the 15° conical nozzle. The lengths from the throat to the exit plane for the 15° conical, 25° conical, and 70 percent contour nozzles were 66.2, 38.6, and 45.4 inches, respectively.

A general digital-computer program for optimum nozzle design available at the Lewis Research Center was used to determine the contour coordinates given in table I. Contours were obtained by the method of characteristics with variable isentropic exponent and shifting-equilibrium gas composition to maximize the thrust coefficient for an area ratio of 100 and a given altitude pressure. Optimum performance for nozzles of several lengths was calculated for a chamber pressure of 60 pounds per square inch absolute and 8.12 percent hydrogen, and a contour was chosen that was equivalent in delivered theoretical performance to a 15° conical nozzle at the same design conditions. The resulting nozzle, referred to as a 70 percent contour, had an exit divergence half-angle of 9° and a maximum-expansion half-angle of 40° near the throat.

Injector

The injector used for the entire program is pictured in figure 3. A 131-element, coaxial-injection pattern was used, each element providing a stream of fluorine surrounded by an annulus of gaseous hydrogen. High pressure drops through the injector favored stable combustion, and at no time were instabilities encountered. Approximately 11 minutes of accumulated running time with the same injector resulted in only discoloration of the thick, copper injector face.

Instrumentation

Locations of all instrumentation are shown in figure 1.

Thrust. - A strain-gage load cell, in compression when loaded, was used for the primary-thrust measurement. Prior to each run, the load cell was calibrated against a standard cell by pressurizing an air cylinder. During operation, the signal from the load cell was divided to read out on high-speed digital tape, a direct-recording oscillograph, and a direct-reading strip chart. Since the load cell was located in the capsule with the engine, no elaborate procedure or additional measurements were required for calibration and thrust determination.

Pressure. - Strain-gage-element transducers were used for all pressure measurements, including differential pressures across the flowmeters. Pickups measuring the higher pressures were referenced or vented to capsule pressure or test-chamber pressure when this pressure was negligible in relation to the measured value. Lower range pressure measurements were referenced to a controlled vacuum system and corrected appropriately. Pressure signals were recorded on a direct-recording oscillograph and on high-speed digital tape. Pickup and recording circuits were calibrated electrically prior to each day of operation by introducing a "calibrate resistance" to correspond to full-scale values. Periodic calibration by application of pressure verified the electrical calibrations.

Temperatures. - Calibrated iron-constantan thermocouples were used for temperature measurements in the gaseous-hydrogen system.

PROCEDURE

Fluorine Handling

Fluorine is the most powerful, stable oxidizing element and is spontaneously combustible with many materials. These two properties caused many test-equipment failures in the early stages of fluorine technology because of improper materials and poor system preparation and handling techniques. This situation, coupled with the physiological effects caused by contact with or inhalation of fluorine or hydrogen fluoride gas, has precipitated much criticism of all proposed programs involving fluorine.

Procedures, for the safe, confident usage of fluorine have been firmly established at the Lewis Research Center, however, through a considerable amount of experience in material compatibility and rocket-engine testing. Preparation of a facility or system for the use of fluorine, including cleaning, drying, and passivating, is thoroughly discussed in references 6 and 7.

Transfer. - Transfer of liquid fluorine from the portable trailer-mounted Dewar (5000-lb capacity) to the propellant tank in the test section was originally accomplished by pressurization of the trailer with helium. This operation was later revised to the following procedure, which was considered safer. The propellant tank in the test chamber was cooled with its liquid-nitrogen bath and then evacuated with a vacuum pump. Fluorine was then transferred by boiling from the trailer at atmospheric pressure into the low-pressure propellant tank and condensing on the cold walls. The quantity transferred was controlled by time, which, in turn, is a function of condensation rate and initial vacuum. This method avoided pressurization of the trailer and minimized the hazard of spillage from a primary failure.

Disposal. - Because of the small quantities of fluorine and hydrogen fluoride involved, adequate disposal was possible by simply diluting the exhaust products with air and providing good dispersal conditions at the exit of the facility. Before entering the facility compressors, the exhaust products, flowing at a maximum rate of 3.5 pounds per second, were diluted with air flowing at approximately 50 pounds per second. The exhaust gases were then pumped to the atmosphere by an ejector using air at 100 pounds per second as the primary flow. This total combined dilution, plus the vertical efflux from the ejector, was sufficient for safe disposal. A more comprehensive discussion of this problem appears in reference 8.

Engine Operation

Control system. - Valve positions for both the fluorine and hydrogen weight flows were controlled by manually preset variable potentiometers. Closed-loop systems to control chamber pressure and mixture ratio to the desired conditions were not used so as to avoid any system instability. The potentiometers and valves were calibrated, and settings for run conditions were determined from flow rates calculated from estimated combustion efficiency.

Operational sequence. - The instrumentation systems, safety systems, and engine firing were all controlled automatically by a program timer. The propellant systems and engine were purged with helium before and after each firing. The required fuel lead and override time was only several milliseconds since the thrust chambers were not cooled by fuel. Immediately following each run, the capsule surrounding the engine was purged with gaseous nitrogen to prevent recirculation of hot, corrosive exhaust gases around the instrumentation and wiring located there. The length of each run varied from 5 to 6 seconds at a chamber pressure of 60 pounds per square inch absolute to 11 to 12 seconds at 10 pounds per square inch absolute. Cooling time required between runs was approximately 10 minutes.

Run conditions. - The initial program called for running each of the three nozzles over a range of mixture ratios from 6 to 12 percent hydrogen at chamber pressures of 60, 40, 20, and 10 pounds per square inch absolute. Difficulty was encountered, however, in establishing full nozzle flow at 20 and 10 pounds per square inch absolute with the 25° conical and 70 percent contour nozzles because of the exhaust-diffuser design. As a result, performance for these two nozzles was obtained only at 60 and 40 pounds per square inch absolute.

RESULTS

All the results are presented in table II to facilitate interpretation and correlation of the performance figures.

Effect of Mixture Ratio

Figure 4(a) shows the performance of the three area-ratio-100 rocket engines operated at a chamber pressure of 60 pounds per square inch absolute over a mix-

ture-ratio range from 12 to 6 percent hydrogen. Maximum impulse over the range tested was obtained at approximately 11 to 12 percent hydrogen for each of the engines. With the 15° conical nozzle, a vacuum specific impulse of 465 seconds was attained, while the 70 percent contour and 25° conical nozzles produced 440 and 430 seconds, respectively, at this condition. As the mixture ratio was varied toward stoichiometric (5.04 percent hydrogen), the impulse performance decreased significantly. At 6 percent hydrogen, for example, the vacuum specific impulse with the 15° nozzle was 434 seconds; the two shorter nozzles produced similar results.

The exhaust-nozzle performance, as measured by vacuum thrust coefficient, was relatively insensitive to variation in mixture ratio for all the nozzles tested. The thrust coefficient of the 15° conical nozzle was 1.88 at the mixture ratio corresponding to maximum impulse performance and varied to 1.92 at a mixture ratio of 6 percent hydrogen. Values at maximum impulse for the 70 percent contour and the 25° conical nozzles were 1.78 and 1.74, respectively.

Combustion performance, as indicated by characteristic velocity c^* diminished rapidly when fuel concentrations were decreased from 12 to 6 percent hydrogen (fuel rich to near stoichiometric). Maximum impulse at a chamber pressure of 60 pounds per square inch absolute was obtained with a characteristic velocity of 8000 feet per second, whereas c^* was only 7300 feet per second at a mixture ratio of 6 percent hydrogen.

Thus, the lower impulse performance near stoichiometric was attributed primarily to combustion performance when the parameters entering into specific impulse were examined individually ($I \times g = c^* \times C_F$). A comparison, however, with the theoretical equilibrium calculations indicated some potential for performance improvement in both the combustion chamber and the exhaust nozzle, particularly at mixture ratios near stoichiometric.

Figure 4(b) shows the performance with the three nozzles at a chamber pressure of 40 pounds per square inch absolute. Values of vacuum specific impulse, vacuum thrust coefficient, and characteristic velocity were very similar to those at 60 pounds per square inch absolute. It should be noted that the composite curve of combustion-chamber performance c^* faired through the majority of points does not accurately represent the data for the 15° conical nozzle for one set of runs (six data points). Later runs with this engine, however, were in agreement with the composite results, and indications pointed to incorrect chamber-pressure readings for this set. For this reason, the thrust-coefficient data for the 15° conical nozzle were considered to be more realistic if represented by a curve utilizing the composite c^* results from all the runs at this chamber pressure, since $C_F \times c^* = I \times g$.

At chamber pressures below 40 pounds per square inch absolute, fully expanded nozzle flow could not be established with the 25° conical and 70 percent contour nozzles with the existing exhaust diffuser. Several procedures were attempted for operation in this region, but none was successful. As a result, figures 4(c) and (d) show nozzle data from just the 15° conical nozzle but characteristic velocity from all tests at the lower pressures. At chamber pressures of 20 and 10 pounds per square inch absolute, the maximum values of specific impulse

were approximately 450 and 440 seconds, respectively. Characteristic velocity was considerably lower at these pressures having a value of 7300 feet per second at 12 percent hydrogen and 10 pounds per square inch absolute. The absolute value of thrust coefficient was unchanged at these lower pressure levels, the nominal value being 1.93 at 10 pounds per square inch absolute; the absolute value also insensitive to changes in mixture ratio over the range investigated.

At no time in the program were problems encountered with combustion instability.

Effect of Chamber Pressure

Figure 5 illustrates the effect of chamber pressure on delivered performance efficiency at a mixture ratio for maximum impulse of 11.7 percent hydrogen. Theoretical data for frozen expansion are also included for comparison. Both the experimental and theoretical frozen data are expressed as a percentage of theoretical equilibrium with one-dimensional flow.

With the 15° conical nozzle, the impulse efficiency was 96 percent of theoretical performance at pressures of 60 and 40 pounds per square inch absolute but decreased to 91 percent at 10 pounds per square inch absolute. Chamber-pressure effects with the 70 percent contour and 25° conical nozzles were not completely evaluated because of the operational problems discussed previously. Impulse efficiency at chamber pressures of 60 and 40 pounds per square inch absolute was 91 percent with the contoured nozzle and only 88 percent with the 25° conical one. Although this indicated that the two shorter nozzles tend toward frozen theoretical performance, the actual chemistry of the expansion process must consider only the nozzle performance and not a composite of nozzle and combustion efficiency. This will be clarified in the DISCUSSION.

Characteristic-velocity efficiency was 98 percent or better with this chamber-injector configuration at 60 and 40 pounds per square inch absolute but was reduced to 92 percent when the engine was throttled over a 6:1 pressure range to 10 pounds per square inch absolute. Considerably lower combustion efficiencies were measured at leaner hydrogen concentrations over the entire pressure range. Unpublished data from other tests at the Lewis Research Center, however, have shown that c^* values of approximately 98 percent of theoretical equilibrium can be maintained over this pressure range with a fixed-area injector of an improved design.

The evaluation of nozzle thrust coefficient showed little change in exhaust-nozzle efficiency over the chamber-pressure range from 60 to 10 pounds per square inch absolute. The 15° conical nozzle maintained a near-equilibrium efficiency of 98 percent of theoretical equilibrium at all pressures, whereas the 70 percent contour and 25° conical nozzles operated at approximately 92 and 89 percent, respectively.

The insensitivity of nozzle performance to chamber pressure (within the range investigated) lends itself well to a hydrogen-fluorine engine that can be throttled. It is believed that, with a suitable optimization program, an engine could be built to deliver an impulse efficiency of at least 96 percent of theo-

retical equilibrium over a throttling range of chamber pressure from 60 to 10 pounds per square inch absolute.

DISCUSSION

The performance of the three nozzles shown in figure 5 indicates the actual percent of theoretical thrust coefficient available for useful propulsion. The 15° conical nozzle, which produced near-equilibrium performance, had impulse efficiencies 5 to 8 percent higher than the other two nozzles. The results indicate that the use of shorter nozzles must come at some sacrifice in performance and that the contouring of the nozzle to 70 percent by normal methods did not recover the losses significantly. This exchange of performance, for reduced nozzle length may be justified, however, for specific missions.

An effort was made to identify the various nozzle losses so that the degree of recombination could be somewhat isolated and could be recognized from general performance measurements. The most significant of these losses that detract from theoretical-equilibrium performance was the nonaxial, or divergent, component of the exhaust gases at the nozzle exit. The geometrical divergence loss was 4.7 percent for the 25° conical nozzle, 1.7 percent for the 15° conical nozzle, and 0.6 percent for the contoured nozzle (9° exit angle). Attempts to evaluate other possible losses, such as viscous effects, shock waves, and heat transfer, resulted in no significant contribution toward explaining the differences between nozzles.

Figure 6 shows the data from figure 5 with the appropriate geometric divergence correction applied to each nozzle. This correction results in a more realistic comparison of the nozzles in regard to internal performance. The amount of recombination can be estimated from the thrust-coefficient efficiency, which basically considers only nozzle performance. At a mixture ratio of 11.7 percent hydrogen, the 15° conical nozzle produced equilibrium performance for chamber pressures between 60 and 10 pounds per square inch absolute. The two shorter nozzles, however, appeared to produce near frozen flow, an indication that only a relatively small degree of recombination occurred at these conditions. A comparison at mixture ratios closer to stoichiometric would show similar differences between the nozzles but at a lower overall percent of recombined energy, possibly because of the higher temperatures and greater amount of energy in the dissociated form.

Since previous experimental and analytical approaches have not been sufficient to describe the expansion process properly, only trends or potential contributing factors can be set forth to explain the differences between nozzles. In theory, some indication of the deviation from equilibrium flow can be obtained from the product of the chemical reaction time and the quenching rate (rate of temperature decrease) of the exhaust gases (Penner's criteria, ref. 9). Although the reaction-rate constants for the processes in a hydrogen-fluorine rocket are not known, a comparison of the quenching rates on the nozzles tested was attempted. When isentropic-expansion data and the local geometric divergence angles were used, cooling rates in the 25° conical and 70 percent contour nozzles were found to be two to three times greater than in the 15° conical nozzle.

Maximum rates up to 6.0×10^7 °R per second were calculated near the throat for the 70 percent contour nozzle. As a result of these comparisons, it seemed reasonable to assume that a significant deviation from equilibrium flow might have occurred at low area ratios in the two shorter nozzles. From this point, according to Bray's criteria, reference 10, frozen flow would prevail through the remainder of the nozzle since conditions required for equilibrium would never again be met. The end result would be recognized in experiments such as described herein by the loss of thrust due to energy frozen in the dissociated state.

If such an approach could define the maximum allowable expansion rates to forestall dissociation losses in rocket nozzles for several of the high-energy propellant combinations, then nozzle-design optimization programs could determine an accurate trade-off of performance for nozzle length and weight savings.

SUMMARY OF RESULTS

An experimental investigation of the performance of hydrogen and fluorine was conducted in rocket engines having exhaust nozzles with an area ratio of 100. Chamber pressure ranged from 60 to 10 pounds per square inch absolute and mixture ratios from 12 to 6 percent hydrogen. The results were as follows:

1. A vacuum specific impulse of 465 pound-seconds per pound was obtained with a 15° conical nozzle at a chamber pressure of 60 pounds per square inch absolute at a mixture ratio of 11.7 percent hydrogen. This amounted to 96 percent of theoretical equilibrium for a one-dimensional nozzle. A 25° conical nozzle and one contoured to 70 percent of the length of the 15° conical nozzle produced impulse values of 430 and 440 seconds, respectively. These values of specific impulse were obtained with a characteristic-velocity efficiency of 98 percent.

2. A vacuum thrust coefficient of 1.88, or 98 percent of theoretical equilibrium, was achieved with the 15° conical nozzle at the conditions of maximum impulse for a chamber pressure of 60 pounds per square inch absolute. For the 70 percent contour nozzle, the thrust coefficient was 1.78; the 25° conical nozzle gave a value of 1.74. The absolute value of the nozzle thrust coefficient was relatively insensitive to changes in propellant mixture ratio, while the thrust-coefficient efficiency at a chamber pressure of 10 pounds per square inch absolute was unchanged from its value at 60 pounds per square inch absolute for the 15° conical nozzle.

3. Decreased specific-impulse performance at lower chamber pressures and at mixture ratios near stoichiometric was due primarily to reduced values of characteristic velocity. Improved injector design should minimize this problem.

4. Data corrected for nozzle exit divergence angle indicated that values of thrust coefficient were near equilibrium expansion for the 15° conical nozzle at fuel-rich mixture ratios and all chamber pressures. The performance of the two shorter nozzles was near frozen under all conditions investigated.

5. Nozzles shorter than the 15° conical nozzle suffered losses that appear to be attributable to chemical kinetics; that is, a failure of the recombination

process because of the high expansion rates. Contour designs for hydrogen-fluorine nozzles should consider finite reaction rates to obtain truly optimum performance.

Lewis Research Center
National Aeronautics and Space Administration
Cleveland, Ohio, April 12, 1963

[redacted]

APPENDIX A

SYMBOLS

A	area, sq in.
C_F	thrust coefficient
c^*	characteristic velocity, ft/sec
D	diameter, in.
F	thrust, lb
g	gravitational conversion factor, 32.2 ft/sec^2
I	specific impulse, (lb)(sec)/lb
L	length, in.
L^*	characteristic length, chamber volume/throat area, in.
$\dot{m}$	mass flow, $\dot{W}/g$, (lb)(sec)/ft
P	pressure, total unless otherwise indicated, lb/sq in.
V	velocity, ft/sec
V_i	resultant injection velocity, $\frac{(\dot{W}V)_{H_2} + (\dot{W}V)_{F_2}}{\dot{W}_{H_2} + \dot{W}_{F_2}}$, $\frac{ft}{sec}$
$\dot{W}$	propellant weight flow, total unless otherwise indicated, lb/sec
α	half-angle of nozzle divergence
λ	nozzle divergence correction factor, $(1 + \cos \alpha)/2$

Subscripts:

a	ambient
c	combustion chamber
e	nozzle exit
ej	exhaust diffuser
ejt	exhaust diffuser throat
eq	shifting equilibrium theoretical

[redacted]

F_2	fluorine or fluorine propellant system
H_2	hydrogen or hydrogen propellant system
i	injector or injection conditions
m	measured
n	nozzle entrance
s	static
t	nozzle throat
vac	vacuum
x	experimental

APPENDIX B

PERFORMANCE CALCULATIONS

Theoretical

The calculation of theoretical data for liquid hydrogen and liquid fluorine, described in reference 11, was carried out in a general program written for an IBM 704 computer.

Calculations were based on the usual assumptions of perfect gas law, adiabatic combustion at constant pressure (nozzle-inlet total pressure), isentropic expansion, no friction, homogeneous mixing, and one-dimensional flow.

The theoretical parameters were expressed as vacuum specific impulse and vacuum thrust coefficient in order to establish a common point of comparison between different nozzles and between different operating conditions of the altitude facility. These parameters are defined in terms of the thrust developed by an engine of finite area ratio firing one dimensionally in a vacuum.

Theoretical performance calculations with liquid fluorine and gaseous hydrogen were made at several conditions to determine the error involved when the enthalpy difference between liquid hydrogen at saturation and gaseous hydrogen at ambient temperature is ignored. At a pressure of 60 pounds per square inch absolute, the vacuum specific impulse with gaseous hydrogen is 0.8 percent higher than that with liquid hydrogen at a mixture ratio of 6.22 percent hydrogen and 2.0 percent higher at 11.7 percent hydrogen. No experimental efficiencies were based on these numbers using gaseous hydrogen.

Experimental

The experimental results designated "delivered" vacuum specific impulse or vacuum thrust coefficient were calculated according to the following methods. Corrections for nonaxial, or divergent, exhaust gases were not included in the calculations for delivered performance. Also, no corrections were made for the counteracting effects of ambient temperature hydrogen and the loss of heat to the solid chamber walls and exterior surroundings.

Chamber pressure. - The calculations of performance parameters are based on the total pressure at the entrance to the nozzle, but, in this program, it was more convenient to measure the pressure at the injector face. A correction was, therefore, calculated to account for the loss in total pressure that was required to accelerate the gases to nozzle-inlet velocity in a constant-area chamber. The following equation is derived from the conservation of momentum with the assumption that pressures are uniform, flow is frictionless, and combustion is completed at the nozzle entrance:

$$\frac{P_{c,i,x}}{P_{c,n,x}} = \left(\frac{P_{c,n,s}}{P_{c,n}}\right) + \frac{I_n g - V_i}{c^*(A_c/A_t)} \qquad \text{(B1)}$$

Solved for chamber pressure, the equation is

$$P_{c,n,x} = \frac{P_{c,i,x}}{\left(\frac{P_{c,n,s}}{P_{c,n}}\right) + \frac{I_n g - V_i}{c^*(A_c/A_t)}} \tag{B2}$$

This equation utilizes the experimental conditions for chamber pressure at the injector face, average experimental injection velocity of the incoming propellants, and the theoretical parameters for I_n, c^*, and $(P_{c,n,s}/P_{c,n})$.

The latter terms imply that flow must be isentropic and maintain equilibrium in the subsonic or converging portion of the nozzle.

Characteristic velocity. - The experimental characteristic velocity based on the corrected nozzle inlet total pressure was then obtained by using the equation

$$c^*_{n,x} = \frac{P_{c,n,x} A_t g}{\dot{W}} \tag{B3}$$

Vacuum thrust. - The measurement of thrust for this program was simplified by the complete encapsulation of the engine and load cell. The only forces exerted on the nozzle were due to the internal pressures governed by the accelerated gases and a single external pressure existing within the capsule acting on the outside of the engine and nozzle. This pressure was assumed to be constant throughout the capsule. The general equation for the thrust of a rocket is

$$F_m = \dot{m}_e V_e + (P_e - P_a) A_e$$

or

$$F_m = (\dot{m}_e V_e + P_e A_e) - P_a A_e \tag{B4}$$

where F_m represents the entire thrust developed at the altitude corresponding to P_a and measured by the load cell. The thrust developed in a vacuum is

$$F_{vac,x} = F_m + P_a A_e \tag{B5}$$

This has the effect of setting the altitude pressure P_a equal to zero in equation (B4).

Vacuum thrust coefficient. - Vacuum thrust (eq. (B5)) and nozzle-inlet total pressure (eq. (B2)) were used to define vacuum thrust coefficient as follows:

$$C_{F,vac,x} = \frac{F_{vac,x}}{P_{c,n,x} A_t} \tag{B6}$$

Vacuum specific impulse. - Experimental vacuum specific impulse was calculated by using vacuum thrust and total propellant weight flow with the relation

$$I_{vac,x} = \frac{F_{vac,x}}{\dot{W}} = \frac{c^*_{n,x} C_{F,vac,x}}{g} \qquad (B7)$$

Solved for chamber pressure, the equation is

$$P_{c,n,x} = \frac{P_{c,i,x}}{\left(\frac{P_{c,n,s}}{P_{c,n}}\right) + \frac{I_n g - V_i}{c^*(A_e/A_t)}} \tag{B2}$$

This equation utilizes the experimental conditions for chamber pressure at the injector face, average experimental injection velocity of the incoming propellants, and the theoretical parameters for I_n, c^*, and $(P_{c,n,s}/P_{c,n})$.

The latter terms imply that flow must be isentropic and maintain equilibrium in the subsonic or converging portion of the nozzle.

Characteristic velocity. - The experimental characteristic velocity based on the corrected nozzle inlet total pressure was then obtained by using the equation

$$c^*_{n,x} = \frac{P_{c,n,x} A_t g}{\dot{W}} \tag{B3}$$

Vacuum thrust. - The measurement of thrust for this program was simplified by the complete encapsulation of the engine and load cell. The only forces exerted on the nozzle were due to the internal pressures governed by the accelerated gases and a single external pressure existing within the capsule acting on the outside of the engine and nozzle. This pressure was assumed to be constant throughout the capsule. The general equation for the thrust of a rocket is

$$F_m = \dot{m}_e V_e + (P_e - P_a) A_e$$

or

$$F_m = (\dot{m}_e V_e + P_e A_e) - P_a A_e \tag{B4}$$

where F_m represents the entire thrust developed at the altitude corresponding to P_a and measured by the load cell. The thrust developed in a vacuum is

$$F_{vac,x} = F_m + P_a A_e \tag{B5}$$

This has the effect of setting the altitude pressure P_a equal to zero in equation (B4).

Vacuum thrust coefficient. - Vacuum thrust (eq. (B5)) and nozzle-inlet total pressure (eq. (B2)) were used to define vacuum thrust coefficient as follows:

$$C_{F,vac,x} = \frac{F_{vac,x}}{P_{c,n,x} A_t} \tag{B6}$$

Vacuum specific impulse. - Experimental vacuum specific impulse was calculated by using vacuum thrust and total propellant weight flow with the relation

REFERENCES

1. Henneberry, H. M., Moseson, M. L., and Himmel, S. C.: Comparison of High Energy Propellants in Final Stages. Paper Presented at IAS Prop. Meeting, Cleveland (Ohio), Mar. 6, 1959.

2. Valentine, Harold H., Burley, Richard R., and Coleman, Ronald S.: Analysis of High-Energy Upper Stages for Solar-Probe Missions. NASA TM X-478, 1962.

3. Burry, R. V., Jortner, J., and Rosemary, J. K.: High Energy Propellant Comparisons for Space Missions. ARS Jour., vol. 31, no. 5, May 1961, pp. 609-613.

4. Jones, William L., Aukerman, Carl A., and Gibb, John W.: Experimental Performance of a Hydrogen-Fluorine Rocket Engine at Several Chamber Pressures and Exhaust-Nozzle Expansion Area Ratios. NASA TM X-387, 1960.

5. Jones, William L., Price, Harold G., Jr., and Lorenzo, Carl F.: Experimental Study of Zero-Flow Ejectors Using Gaseous Nitrogen. NASA TN D-203, 1960.

6. Schmidt, Harold W., and Rothenberg, Edward A.: Some Problems in Using Fluorine in Rocket Systems. Proc. Propellant, Thermodynamics and Handling Conf., Spec. Rep. 12, Eng. Experiment Station, Ohio State Univ., June 1960, pp. 183-202.

7. Engineering Department: Launch Area Servicing of a Fluorine Hydrogen Upper Stage. Rep. 8031-982-003, Bell Aerosystems Co., Dec. 31, 1960.

8. Wilcox, Fred A., and Bloomer, Harry E.: Handling Rocket Exhaust Products in Altitude Facilities. Paper Presented at Symposium on Rocket Operation at Simulated High Altitudes and in Space, Tullahoma (Tenn.), June 28-29, 1961.

9. Penner, S. S.: Introduction to the Study of Chemical Reactions in Flow Systems. Agardograph 7, Butterworths Sci. Pub. (London), 1955.

10. Bray, K. N. C.: Atomic Recombination in a Hypersonic Wind-Tunnel Nozzle. Jour. Fluid Mech., vol. 6, July 1959, pp. 1-32.

11. Zeleznik, Frank J., and Gordon, Sanford: A General IBM 704 or 7090 Computer Program for Computation of Chemical Equilibrium Compositions, Rocket Performance, and Chapman-Jouguet Detonations. NASA TN D-1454, 1962.

TABLE I. - COORDINATES FOR 70 PERCENT CONTOUR NOZZLE

[Dimensions in inches.]

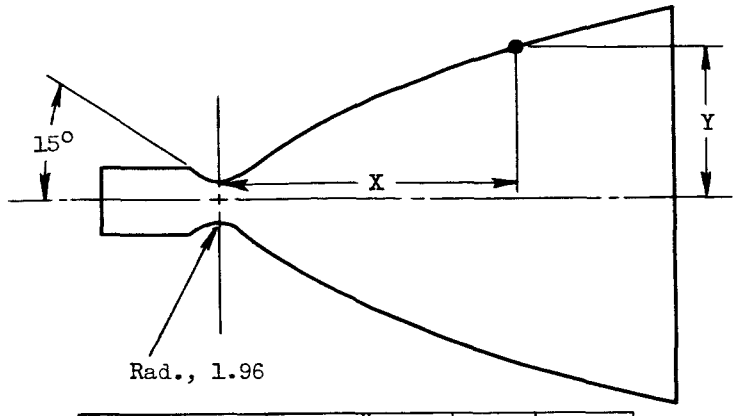

X	Y	Area ratio, ϵ	X	Y	Area ratio, ϵ
-12.91	2.70	1.91	22.00	13.33	46.50
-3.02	2.70	1.91	23.00	13.67	48.95
[a]-.50	[a]2.02	[a]1.07	24.00	14.02	51.45
0	1.955	1.00	25.00	14.34	53.90
[a]1.26	[a]2.42	[a]1.53	26.00	14.67	56.30
1.50	2.62	1.80	27.00	14.97	58.65
2.00	3.02	2.39	28.00	15.28	61.20
2.50	3.41	3.04	29.00	15.56	63.40
3.00	3.78	3.74	30.00	15.85	65.75
3.50	4.15	4.51	31.00	16.13	68.10
4.00	4.51	5.32	32.00	16.40	70.35
4.50	4.86	6.18	33.00	16.67	72.80
5.00	5.20	7.07	34.00	16.93	75.00
5.50	5.53	8.00	35.00	17.18	77.20
6.00	5.85	8.95	36.00	17.43	79.50
7.00	6.48	10.99	37.00	17.68	81.80
8.00	7.08	13.12	38.00	17.92	84.10
9.00	7.65	15.31	39.00	18.17	86.45
10.00	8.19	17.55	40.00	18.39	88.50
11.00	8.71	19.85	41.00	18.62	90.75
12.00	9.21	22.19	42.00	18.83	92.80
13.00	9.69	24.57	43.00	19.05	94.95
14.00	10.15	26.95	44.00	19.26	97.10
15.00	10.60	29.40	45.00	19.47	99.15
16.00	11.03	31.83	45.39	19.55	100.0
17.00	11.44	34.24			
18.00	11.84	36.67			
19.00	12.22	39.07			
20.00	12.60	41.55			
21.00	12.97	44.00			

[a]Tangent point.

TABLE II. - ROCKET ENGINE PERFORMANCE WITH LIQUID FLUORINE AND GASEOUS HYDROGEN

Nozzle	Experimental data									Experimental efficiency			Theoretical values			Basic parameters				
	Nozzle throat area, A_t, sq in.	Chamber pressure, $P_{c,n,x}$, lb/sq in. abs	Mixture ratio: Hydrogen, percent	Mixture ratio: Oxidant-fuel ratio	Total propellant flow rate, W, lb/sec	Total vacuum thrust, $F_{vac,x}$, lb	Characteristic velocity, $c^*_{n,x}$, ft/sec	Vacuum thrust coefficient, $C_{F,vac,x}$	Vacuum specific impulse, $I_{vac,x}$, lb-sec/lb	$c^*_{n,x}/c^*_{n,eq} \times 100$, percent	$C_{F,vac,x}/C_{F,vac,eq} \times 100$, percent	$I_{vac,x}/I_{vac,eq} \times 100$, percent	Vacuum specific impulse, $I_{vac,eq}$, lb-sec/lb	Characteristic velocity, $c^*_{n,eq}$, ft/sec	Vacuum thrust coefficient, $C_{F,vac,eq}$	Momentum correction, $P_{e,}/P_{e,n}$	Vacuum thrust addition, A_eP_e, lb	Hydrogen injector pressure drop, $\Delta P_{H_2,i}$, lb/sq in.	Fluorine injector pressure drop, $\Delta P_{F_2,i}$, lb/sq in.	Run time, sec
Nominal chamber pressure, 60 pounds per square inch absolute																				
15° Conical	11.978	56.1	6.18	15.20	3.01	1313	7200	1.954	436.5	93.5	96.7	90.3	483.6	7700	2.020	1.0456	79.0	21.9	100.4	7.02
		57.4	8.00	11.50	2.97	1352	7450	1.966	458.1	94.6	98.9	93.8	485.4	7870	1.987	1.0422	88.0	36.7	91.0	6.70
	11.959	57.5	10.44	8.58	2.87	----	7711	-----	-----	96.0	----	----	-----	8036	-----	1.0358	----	44.3	75.0	3.00
		57.9	10.02	8.98	2.86	----	7802	-----	-----	97.4	----	----	-----	8012	-----	1.0373	----	44.5	77.4	2.37
		58.4	9.04	10.06	2.93	----	7671	-----	-----	96.5	----	----	-----	7952	-----	1.0394	----	34.6	80.9	5.37
		62.1	6.52	14.35	3.25	----	7347	-----	-----	94.7	----	----	-----	7758	-----	1.0444	----	22.1	105.5	5.00
		61.5	11.09	8.02	3.01	----	7868	-----	-----	97.4	----	----	-----	8082	-----	1.0344	----	50.1	88.7	2.00
	11.903	60.0	10.33	8.68	2.91	1331	7893	1.864	457.2	98.2	95.8	94.1	486.0	8040	1.945	1.0365	52.9	38.8	79.8	4.02
		59.9	9.30	9.75	2.94	1348	7815	1.890	459.3	98.1	96.4	94.6	485.3	7967	1.960	1.0400	57.7	53.7	79.7	1.43
		59.7	7.50	12.34	3.00	1338	7623	1.882	446.1	97.2	94.6	92.0	485.1	7847	1.989	1.0433	63.7	26.0	87.7	5.35
		60.4	5.92	15.90	3.13	1345	7387	1.871	429.6	96.2	92.3	88.9	483.4	7677	2.026	1.0461	63.7	11.3	96.8	5.00
		61.1	12.16	7.22	2.92	1368	8007	1.881	468.2	98.2	98.7	96.9	483.1	8152	1.906	1.0322	44.5	59.9	66.9	6.06
		60.7	10.72	8.32	2.96	1377	7866	1.906	466.0	97.6	98.3	95.9	485.8	8058	1.939	1.0361	42.1	49.1	68.1	8.14
		63.6	11.44	7.74	3.07	1407	7928	1.859	458.0	97.7	96.8	94.6	484.3	8112	1.921	1.0337	55.3	57.3	90.3	2.01
20° Conical	12.023	61.8	12.13	7.25	3.07	1323	7790	1.794	430.8	95.6	93.9	89.2	483.0	8150	1.910	1.0329	55.2	72.7	86.2	5.00
		58.7	10.92	8.42	2.92	1255	7800	1.777	429.8	96.7	91.5	88.6	485.0	8070	1.943	1.0350	52.8	64.0	77.5	5.06
		60.0	9.36	9.67	3.05	1285	7560	1.782	418.4	94.9	90.9	86.3	485.0	7970	1.960	1.0395	61.2	47.2	85.6	5.43
		61.4	6.81	13.70	3.23	1307	7370	1.768	405.0	94.7	88.0	83.5	485.0	7785	2.010	1.0450	58.8	29.0	105.5	5.29
	11.982	58.3	10.52	8.51	2.85	1217	7863	1.748	427.1	97.8	90.0	87.9	485.8	8043	1.943	1.0367	54.0	48.2	77.6	6.17
		61.2	8.43	10.87	3.04	1274	7733	1.743	418.9	97.6	88.5	86.4	485.0	7920	1.970	1.0415	67.2	33.3	89.3	5.13
		62.2	6.39	14.65	3.17	1311	7542	1.763	413.4	97.4	87.6	85.3	484.7	7745	2.013	1.0450	80.4	23.0	103.0	5.06
70 Percent contour	11.897	60.6	8.75	10.43	2.98	1291	7777	1.792	433.2	98.0	91.0	89.1	486.0	7940	1.969	1.0405	91.1	29.2	93.0	2.00
		61.5	11.27	7.87	2.93	1281	8017	1.751	436.6	99.0	91.1	90.2	484.1	8100	1.923	1.0348	62.3	53.8	78.4	5.82
		61.9	10.98	8.11	2.97	1307	7986	1.774	440.5	98.9	91.9	90.9	484.7	8079	1.930	1.0353	76.7	49.8	75.9	4.75
		57.5	6.00	15.65	3.03	----	7269	-----	-----	94.7	----	----	-----	7673	-----	1.0458	----	16.3	94.9	4.47
		61.6	9.21	9.86	3.08	1323	7667	1.805	430.2	96.2	92.0	88.5	485.9	7970	1.961	1.0390	80.3	34.3	89.0	4.50
	11.886	63.4	11.43	7.75	3.01	1307	8075	1.734	435.1	99.6	90.3	89.9	484.0	8108	1.920	1.0340	39.5	56.4	77.4	2.20
		64.1	10.90	8.18	3.07	1353	7986	1.774	440.7	98.9	92.0	91.0	484.5	8078	1.929	1.0355	39.5	59.6	76.6	3.20
	11.914	63.2	11.44	7.74	3.03	1320	8001	1.754	436.4	98.7	91.4	90.2	484.0	8108	1.920	1.0340	39.5	60.7	77.7	5.00
		64.4	10.45	8.57	3.09	1358	7990	1.769	439.5	99.2	91.3	90.6	485.1	8053	1.938	1.0370	39.5	54.7	80.2	2.70
	11.944	61.6	7.74	11.92	3.04	1319	7786	1.791	433.6	98.9	90.2	89.3	485.6	7870	1.985	1.0432	52.7	28.9	85.7	1.80
		61.6	6.62	14.11	3.12	1316	7596	1.788	422.2	97.8	89.1	87.1	484.7	7769	2.007	1.0452	50.3	22.0	90.6	3.10

Nominal chamber pressure, 40 pounds per square inch absolute																			
15° Conical	11.978	42.0	11.29	7.85	2.17	980	7470	1.946	451.2	92.6	100.8	93.3	483.5	8060	1.930	1.0340	61.0	42.8	62.4	3.85
		41.2	11.30	7.85	2.09	976	7610	1.976	466.9	94.4	102.4	96.6	483.5	8060	1.930	1.0348	61.0	45.7	65.1	6.89
		36.4	12.89	6.78	1.84	857	7640	1.964	465.9	94.0	102.8	96.8	481.5	8130	1.910	1.0305	61.0	50.7	51.0	6.88
		39.3	7.82	11.79	2.06	922	7360	1.957	447.8	94.2	98.1	92.4	484.5	7810	1.995	1.0435	61.0	23.2	65.7	6.84
		39.4	5.96	15.79	2.13	916	7140	1.940	430.6	93.5	95.6	89.3	482.0	7640	2.030	1.0472	61.0	15.1	63.9	7.00
		40.0	7.62	12.10	2.10	940	7350	1.961	447.7	94.1	98.1	92.4	484.5	7810	1.998	1.0440	65.0	23.2	63.4	6.35
	11.903	41.3	8.23	11.15	2.07	933	7647	1.898	451.2	97.3	95.8	93.2	484.1	7863	1.981	1.0415	55.3	21.9	49.4	5.47
		40.7	9.44	9.59	2.00	929	7789	1.918	464.3	98.2	97.6	95.8	484.5	7934	1.965	1.0403	54.1	26.6	48.1	6.95
20° Conical	11.882	44.1	9.84	9.16	2.16	882	7788	1.684	407.9	97.8	86.1	84.2	484.3	7962	1.957	1.0387	41.0	36.8	57.2	5.53
		42.2	8.40	10.90	2.09	858	7707	1.711	409.8	97.8	86.2	84.5	484.8	7878	1.948	1.0422	49.0	26.2	53.4	5.58
		40.5	6.26	14.98	2.09	836	7397	1.736	399.3	96.5	85.8	82.8	482.0	7666	2.023	1.0465	48.0	16.4	58.6	5.49
		39.9	6.93	13.44	2.03	823	7496	1.736	405.0	96.7	86.4	83.8	483.3	7750	2.009	1.0454	49.0	19.0	57.0	4.71
		41.2	10.77	8.28	2.04	853	7712	1.742	417.4	96.2	89.7	86.3	483.8	8015	1.942	1.0365	50.0	39.8	49.8	4.57
70 Percent contour	11.897	42.6	12.55	6.97	2.03	918	8059	1.809	453.4	99.1	94.8	94.2	481.4	8135	1.908	1.0320	75.5	41.2	47.6	5.16
		40.2	9.56	9.46	1.97	876	7826	1.857	445.6	98.5	94.7	92.0	484.2	7942	1.961	1.0397	80.3	24.6	46.5	6.42
		41.2	7.99	11.51	2.02	---	7791	-----	-----	99.4	----	----	-----	7838	-----	1.0437	----	19.6	49.7	4.00
		41.4	8.28	11.08	2.03	---	7809	-----	-----	99.3	----	----	-----	7862	-----	1.0439	----	19.6	46.6	2.55
		41.2	6.48	14.42	2.07	---	7610	-----	-----	98.8	----	----	-----	7700	-----	1.0466	----	13.7	53.9	6.51
	11.944	41.8	10.40	8.62	2.04	882	7885	1.764	432.5	98.5	90.5	89.3	484.1	8005	1.949	1.0374	47.9	30.9	48.1	2.70
	11.972	40.7	11.01	8.08	1.94	858	8066	1.762	441.7	100.3	90.9	91.4	483.4	8038	1.938	1.0370	44.3	32.1	50.4	2.60
		42.1	9.10	9.99	2.03	903	8009	1.789	445.5	101.2	90.8	91.9	484.6	7915	1.970	1.0420	45.5	29.0	49.7	1.90
		43.3	7.99	11.52	2.15	955	7767	1.844	445.1	99.1	92.9	91.9	484.5	7840	1.984	1.0445	46.7	25.7	51.3	2.90
	12.036	41.4	6.10	15.38	2.12	900	7579	1.806	425.5	99.1	89.0	88.3	482.1	7646	2.030	1.0483	47.9	11.3	51.2	3.80
Nominal chamber pressure, 20 pounds per square inch absolute																			
15° Conical	11.974	18.1	11.38	7.79	0.965	432	7220	1.995	458.1	90.5	102.4	95.0	482.0	7975	1.948	1.0350	26.4	26.3	52.3	6.27
		19.8	10.41	8.60	1.051	465	7250	1.961	442.4	91.5	100.0	91.6	483.0	7915	1.962	1.0381	25.2	23.5	49.9	6.00
		20.4	8.10	11.34	1.097	476	7160	1.947	434.5	92.1	97.4	90.1	482.5	7770	2.000	1.0441	20.4	16.5	52.7	5.91
		20.2	7.30	12.70	1.100	471	7070	1.946	428.6	91.7	96.8	89.0	481.8	7710	2.010	1.0460	18.0	14.9	50.8	6.00
		19.6	6.27	14.98	1.118	451	6753	1.925	403.4	88.8	94.9	84.5	478.0	7588	2.028	1.0472	14.0	11.7	49.9	6.02
		20.2	11.40	7.75	1.043	469	7460	1.939	449.7	93.4	99.9	93.3	482.0	7984	1.941	1.0368	20.0	28.1	59.0	6.11
		20.1	11.00	8.08	1.036	459	7480	1.917	444.3	94.0	98.3	92.2	482.0	7958	1.950	1.0378	18.0	27.1	59.6	6.47
	12.036	22.9	9.92	9.06	1.172	513	7560	1.859	437.4	95.7	94.5	90.6	483.0	7900	1.967	1.0400	28.9	21.5	44.6	10.75
		20.4	11.56	7.65	1.055	484	7500	1.971	459.1	93.8	101.7	95.2	482.0	8000	1.938	1.0352	28.9	24.4	44.4	10.65
		20.8	8.08	11.37	1.121	483	7180	1.928	430.6	92.4	96.4	89.2	483.0	7770	2.000	1.0431	22.8	3.8	49.1	8.28
		22.4	5.64	16.73	1.198	511	7250	1.891	426.6	96.5	92.6	89.4	477.0	7510	2.043	1.0491	21.6	----	47.9	7.75
20° Conical	11.903	20.3	12.84	6.72	1.020	---	7621	-----	-----	94.3	----	----	-----	8079	-----	1.0308	----	24.1	----	8.51
		20.4	10.36	8.65	1.052	---	7425	-----	-----	93.7	----	----	-----	7922	-----	1.0383	----	21.5	----	8.55
		21.6	9.18	9.89	1.100	---	7519	-----	-----	95.8	----	----	-----	7850	-----	1.0415	----	18.1	----	8.26
		19.9	5.62	16.81	1.122	---	6792	-----	-----	90.8	----	----	-----	7480	-----	1.0488	----	7.1	----	8.53
		21.2	9.72	9.30	1.091	---	7441	-----	-----	94.4	----	----	-----	7885	-----	1.0396	----	17.7	----	11.60
	11.952	21.9	12.35	7.10	1.083	---	7764	-----	-----	96.4	----	----	-----	8052	-----	1.0334	----	27.0	48.8	5.09
Nominal chamber pressure, 10 pounds per square inch absolute																			
15° Conical	11.974	10.6	13.33	6.49	0.566	---	7210	-----	-----	89.7	----	----	-----	8040	-----	1.0300	----	19.2	61.9	5.73
		10.1	11.70	7.55	.546	---	7120	-----	-----	89.8	----	----	-----	7930	-----	1.0355	----	17.5	63.5	5.81
		10.5	10.38	8.63	.565	---	7160	-----	-----	91.3	----	----	-----	7850	-----	1.0391	----	14.1	68.4	7.60
		9.8	8.40	10.90	.563	231	6690	1.975	410.9	86.9	98.5	85.4	481.0	7700	2.010	1.0439	25.0	9.8	63.2	7.45
		9.3	5.09	18.65	.619	---	5598	-----	-----	78.0	----	----	-----	7265	-----	1.0503	----	5.5	58.4	7.70
		9.6	5.51	17.15	.626	---	5720	-----	-----	78.6	----	----	-----	7377	-----	1.0494	----	5.0	64.9	7.55
		10.1	5.85	16.15	.622	---	6080	-----	-----	81.7	----	----	-----	7445	-----	1.0492	----	6.4	63.4	7.50
	12.035	10.6	11.70	7.56	0.546	239	7500	1.875	437.4	94.5	96.2	90.9	481.0	7935	1.950	1.0331	14.4	5.4	51.1	11.40
		11.1	10.60	8.45	.556	245	7700	1.838	440.4	97.9	93.2	91.4	482.0	7860	1.973	1.0372	12.0	4.4	53.4	11.16
		11.4	6.89	13.50	.675	263	6570	1.907	389.3	86.4	93.9	81.1	480.0	7605	2.030	1.0462	12.0	2.0	50.0	11.14
		10.9	6.78	13.73	.657	241	6410	1.839	366.7	84.5	90.5	76.6	479.0	7585	2.032	1.0462	7.2	1.1	52.9	15.27
25° Conical	11.903	9.5	12.45	7.04	0.482	---	7530	-----	-----	94.5	----	----	-----	7968	-----	1.0337	----	13.1	----	11.35
		10.6	9.91	9.09	.575	---	7059	-----	-----	90.4	----	----	-----	7807	-----	1.0394	----	10.7	----	11.54
		10.8	8.31	11.03	.614	---	6741	-----	-----	87.5	----	----	-----	7702	-----	1.0433	----	8.6	----	11.65
		10.6	6.86	13.57	.641	---	6332	-----	-----	83.4	----	----	-----	7590	-----	1.0461	----	6.7	----	11.67

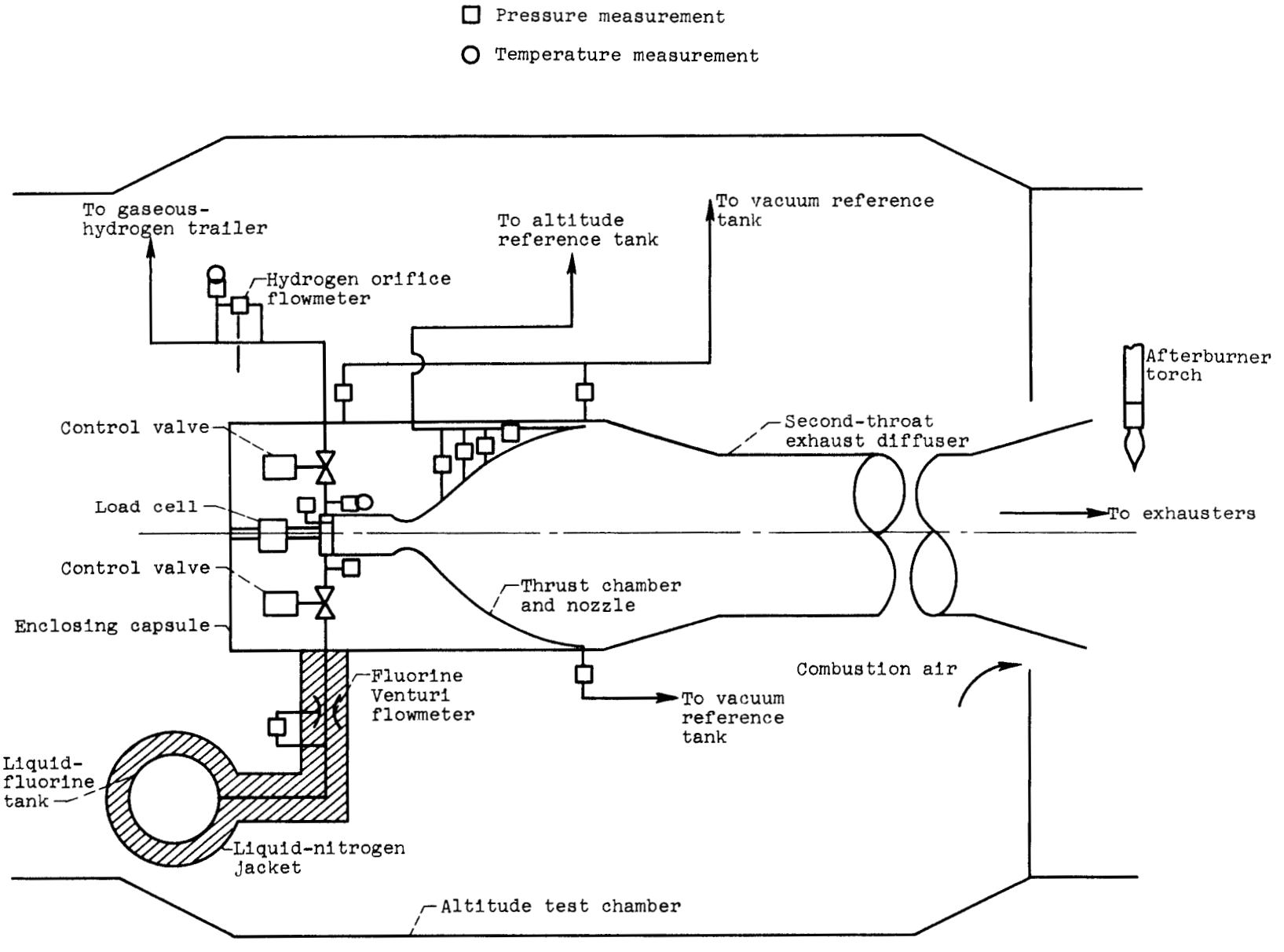

Figure 1. - Test section of altitude facility.

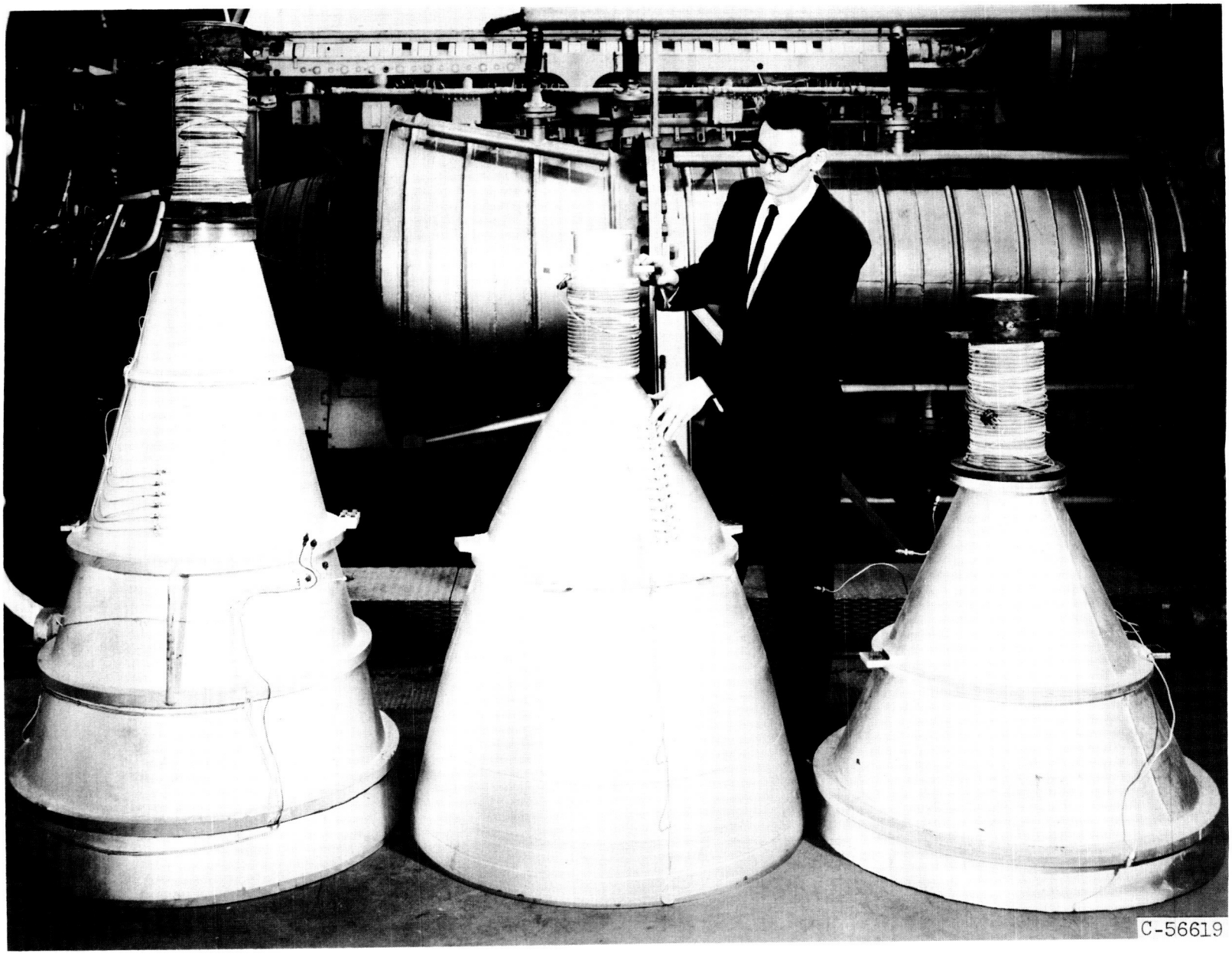

Figure 2. - Three rocket engines with nozzle area ratios of 100.

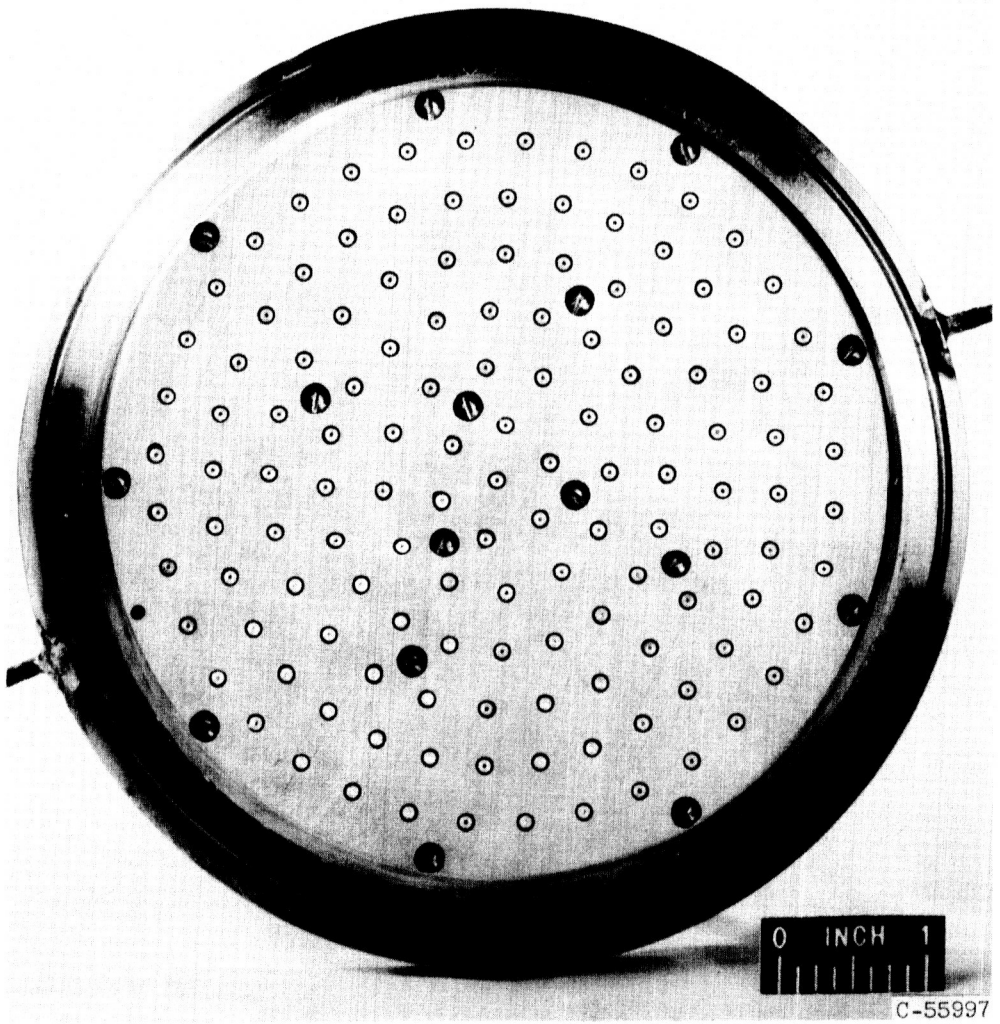

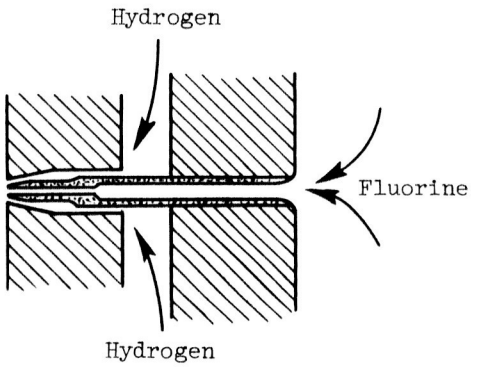

Coaxial injector element

	Fluorine	Hydrogen
Hole diameter, in.	0.025	0.120
Annulus height, in.	-----	0.033
Total area, sq in.	0.0643	0.702

Figure 3. - Coaxial injector with 131 elements.

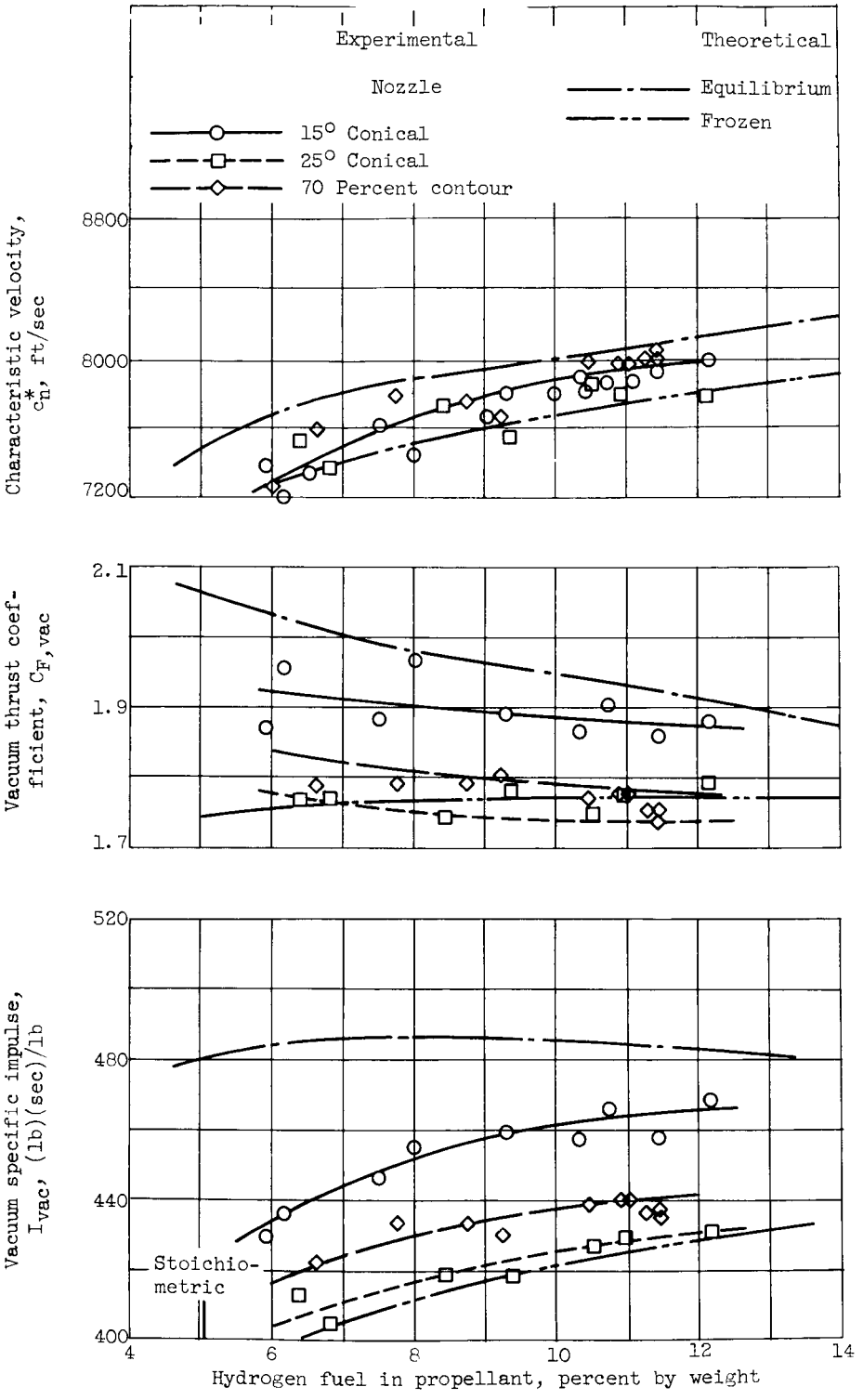

(a) Chamber pressure, 60 pounds per square inch absolute.

Figure 4. - Experimental hydrogen-fluorine rocket performance at area ratio of 100.

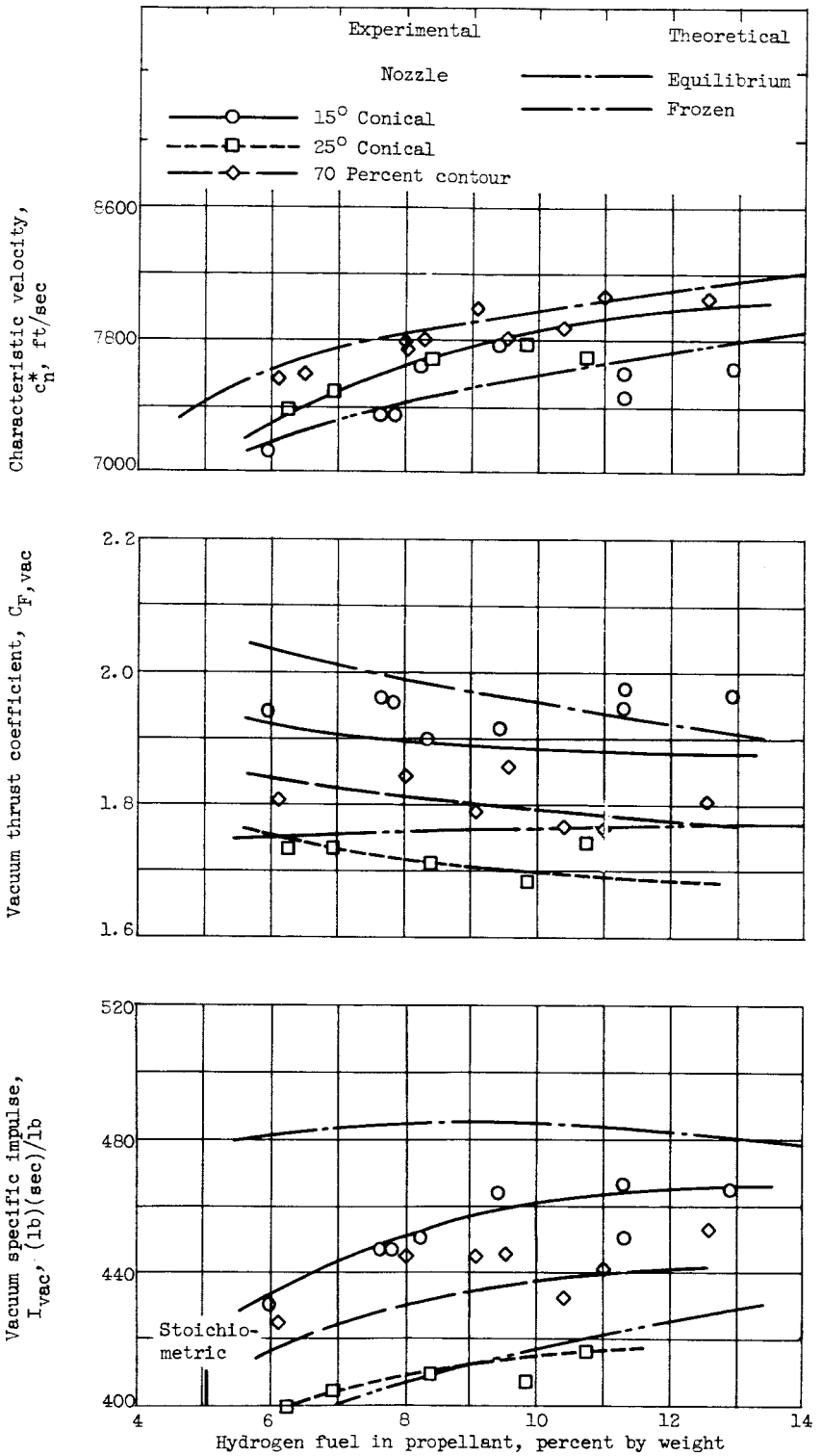

(b) Chamber pressure, 40 pounds per square inch absolute.

Figure 4. - Continued. Experimental hydrogen-fluorine rocket performance at area ratio of 100.

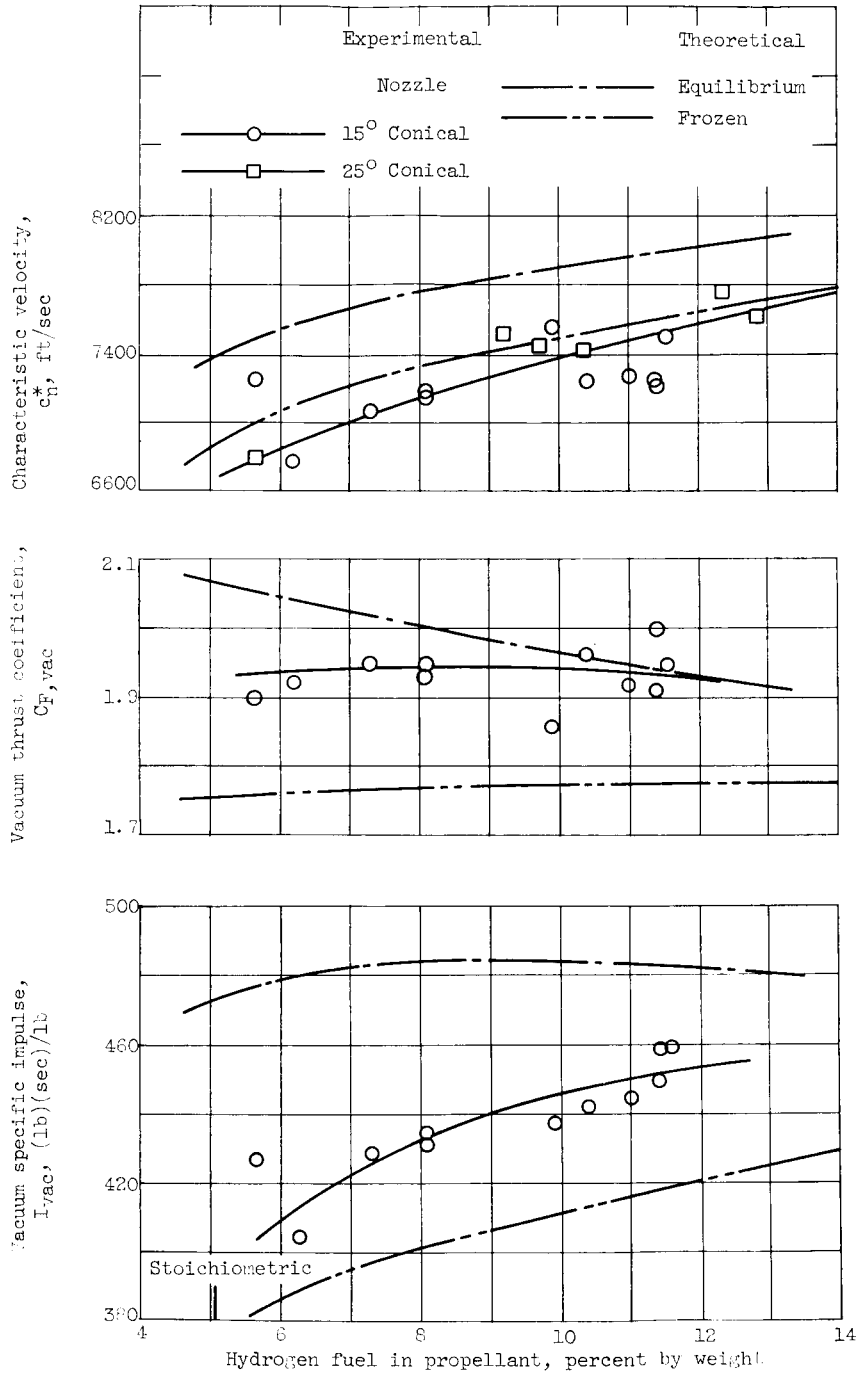

(c) Chamber pressure, 20 pounds per square inch absolute.

Figure 4. - Continued. Experimental hydrogen-fluorine rocket performance at area ratio of 100.

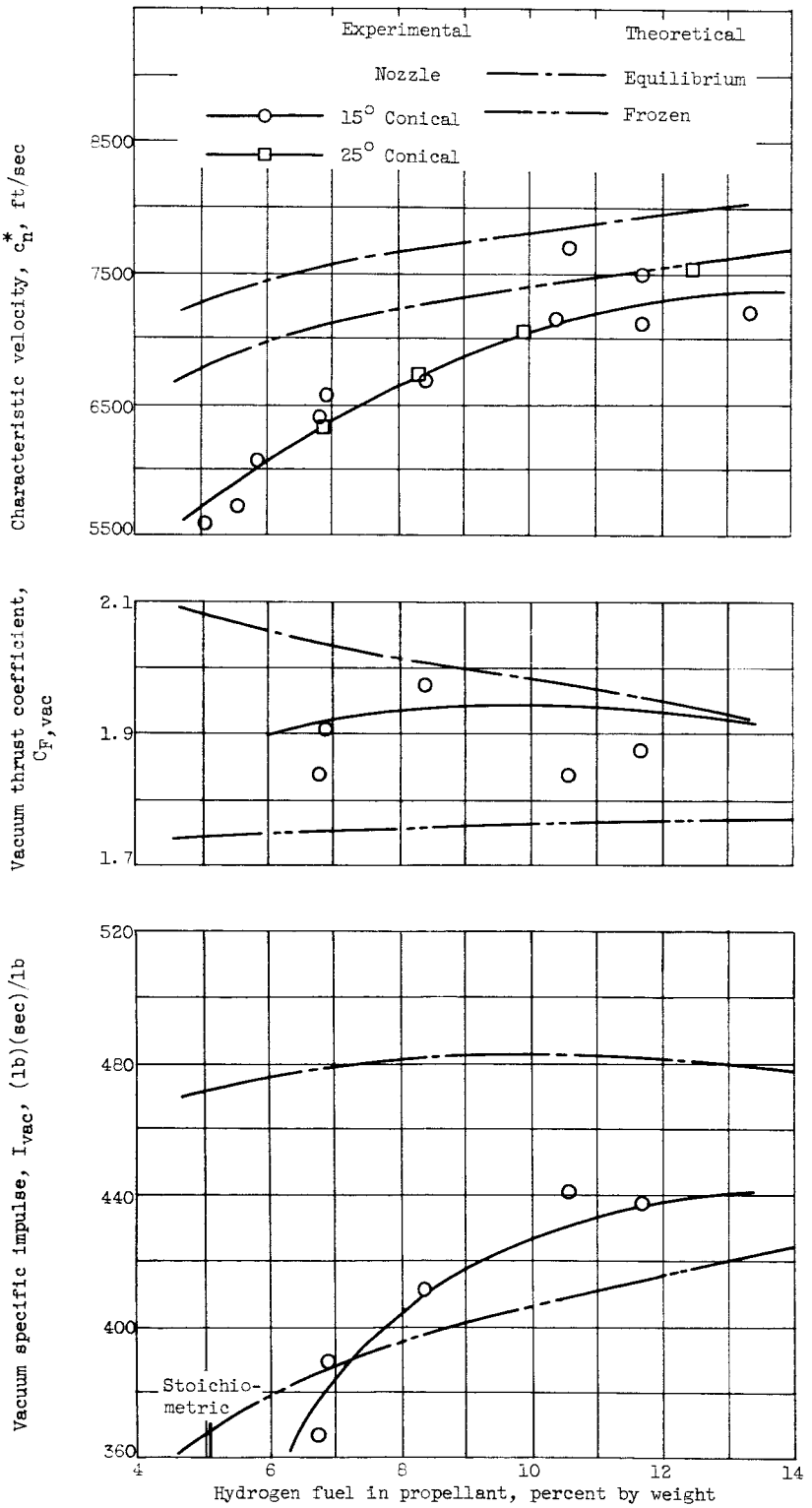

(d) Chamber pressure, 10 pounds per square inch absolute.

Figure 4. - Concluded. Experimental hydrogen-fluorine rocket performance at area ratio of 100.

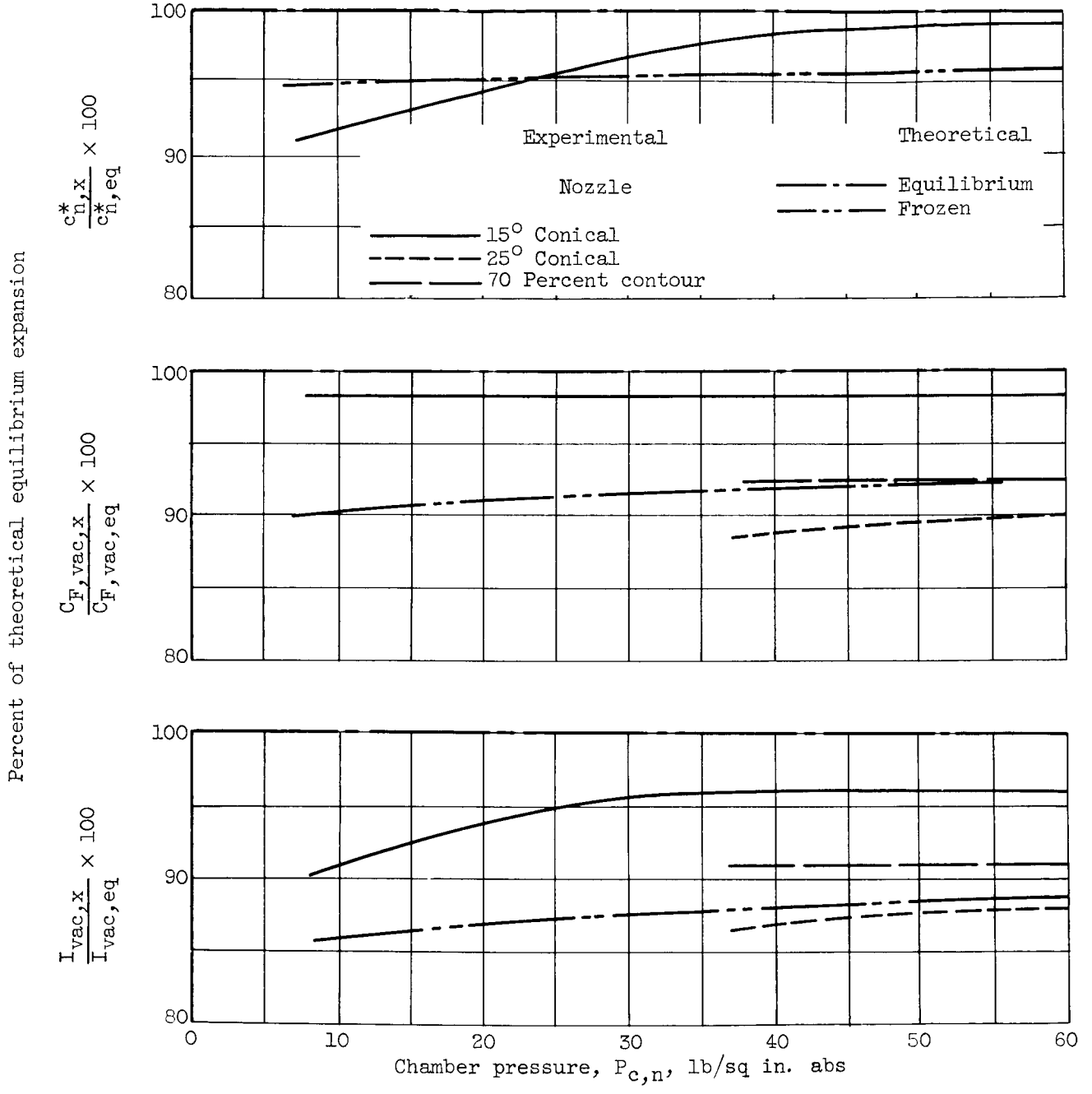

Figure 5. - Effect of chamber pressure on delivered performance efficiency of experimental rocket engine at mixture ratio of 11.7 percent hydrogen and area ratio of 100.

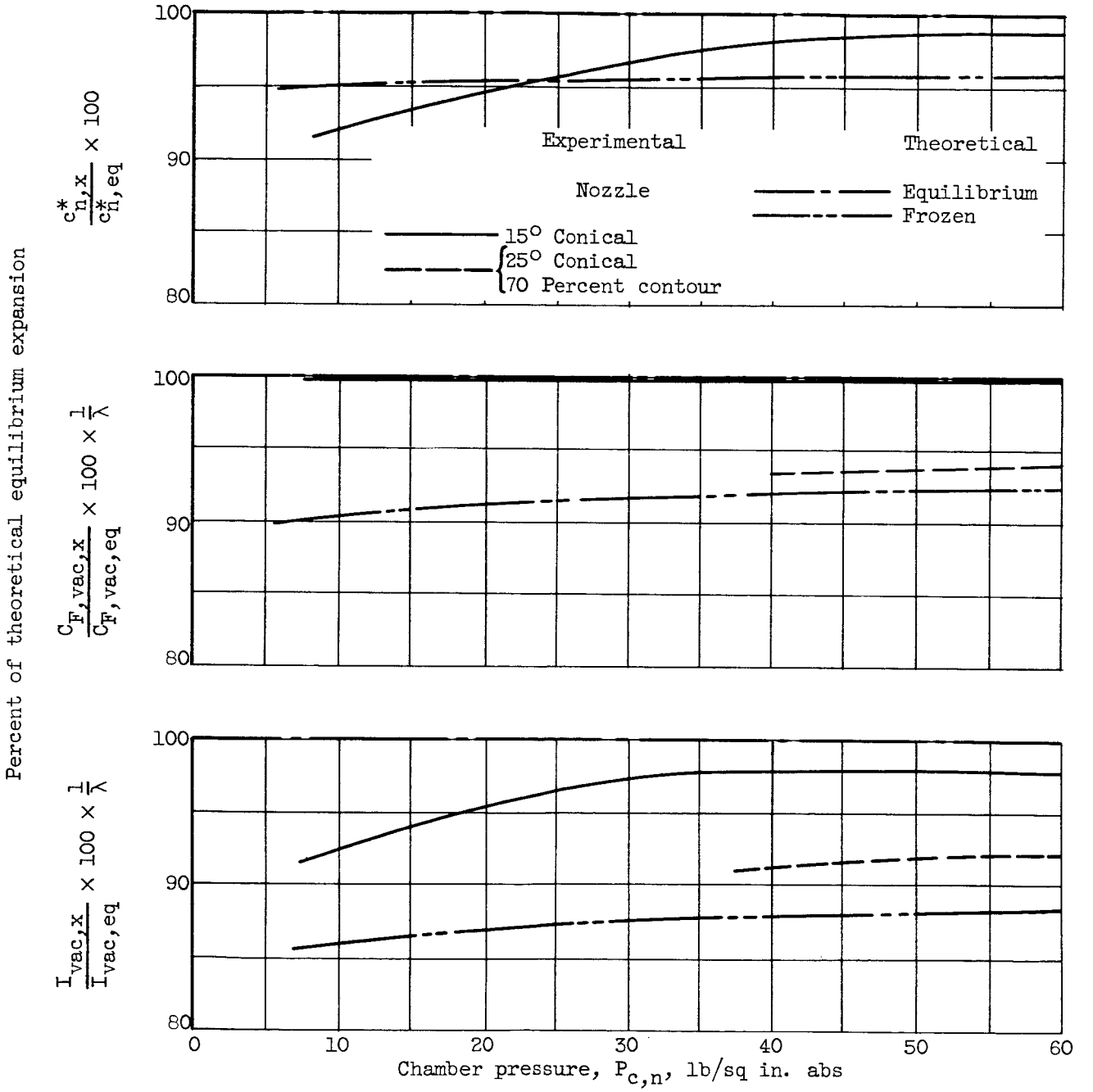

Figure 6. - Experimental nozzle performance efficiency at mixture ratio of 11.7 percent hydrogen and area ratio of 100.